Jurnal Teknik Mesin, Industri, Elektro dan Informatika
Volume 5, Nomor 3, September 2026
e-ISSN: 2963-7805; p-ISSN: 2963-8208, Hal. 34-54
DOI: https://doi.org/10.55606/jtmei.v5i3.6302
Tersedia: https://ejurnal.politeknikpratama.ac.id/index.php/jtmei

Analysis of Carbody Spreader Loading of Electric Rail Train on Material Variations Using Finite Element Analysis Method

Alviz Mahardika Effendi[1*], Muhammad Fuad Abdul Hakim[2], Doni Dwi Susilo[3], Salim Subarkah[4]
[1-3]Mechanical Engineering Study Program, Merdeka University Madiun, Indonesia
[4]Production and Manufacturing Mechanical Engineering, State Polytechnic of Malang, Indonesia
Email: alviz.mahardikaeffendi06@gmail.com[1], muhammadfuad@unmer-madiun.ac.id[2], donidwisusilo3@gmail.com[3], salim.subarkah@polinema.ac.id[4]
**Corresponding Author: alviz.mahardikaeffendi06@gmail.com*

Abstract. This research analyzes the structural strength of an adjustable spreader carbody for Electric Multiple Unit (EMU) trains under a 40-ton load to determine the most optimal and efficient material for manufacturing at PERUSAHAAN KERETA API (Persero). The study employs Finite Element Analysis (FEA) static structural simulation using Ansys Workbench, based on a 3D model created in Autodesk Inventor. The spreader's most critical condition at a 4000 mm length was evaluated across three material variations: SS400, SM490A, and S355J2+N steel. Simulation results indicate that all materials are structurally safe, exhibiting maximum von Mises stresses between 106.96 MPa and 107.18 MPa, well below their respective yield strengths. Total deformation remained minimal at under 0.08 mm, and the minimum safety factors ranged from 2.94 to 3.22, satisfying the industrial standard of 2.5 to 3.0 for lifting equipment. Although S355J2+N offers the highest safety margin, SS400 is identified as the most optimal and efficient choice. It provides an adequate safety factor of 3.011, minimal deformation, superior cost-effectiveness, and broad market availability, ensuring safe and economical lifting operations without compromising structural integrity.

Keywords: Adjustable Spreader Carbody; Electric Multiple Unit (EMU); Finite Element Analysis (FEA); SS400 Material Optimization; Structural Strength Analysis.

1. INTRODUCTION

The Indonesian railway industry, particularly in East Java, serves as a pivotal hub for rolling stock manufacturing in Southeast Asia. As the demand for efficient mass transit grows, the production and logistics of heavy railway components, such as Electric Multiple Unit (EMU) car bodies, require stringent safety and precision standards (Harnany et al., 2024; Kljaić et al., 2023; Zhao et al., 2020). Handling these massive structures, which can weigh up to 40 tons, necessitates specialized lifting equipment to prevent structural damage and ensure operational safety during transportation from production lines to assembly areas.

In this logistical process, the adjustable spreader beam plays a crucial role in distributing the concentrated load of the car body evenly to the crane's lifting mechanism. The spreader must withstand significant dynamic and static loads without experiencing excessive deformation or structural failure. However, current practices in selecting spreader materials often lack a proportional consideration of economic efficiency and weight optimization. Suboptimal material selection can lead to unnecessarily heavy equipment, inflated production costs, or compromised safety margins during repetitive lifting operations (Oswald et al., 2020; Tang et al., 2026; Wokanubun et al., 2023).

Received: 26 April 2026; Revised: 25 May 2026; Accepted: 20 June 2026; Available: 30 June 2026

The structural integrity of lifting equipment is highly dependent on the mechanical properties of the chosen material. Structural steels, such as SS400, SM490A, and S355J2+N, are commonly utilized due to their high tensile strength and ductility. Nevertheless, the variation in yield strength and modulus of elasticity among these materials directly influences the stress distribution and deflection of the spreader under maximum load conditions. Therefore, a comprehensive evaluation is required to balance the technical requirements of high load-bearing capacity with the economic imperatives of manufacturing (Efinger et al., 2022; Pierce & Henriksen, 2022; Xu et al., 2025).

To address these engineering challenges without the high costs of physical prototyping, Finite Element Analysis (FEA) has become an indispensable tool in mechanical design optimization. By utilizing 3D modeling software integrated with computational solvers, engineers can accurately simulate real-world loading conditions, predict stress concentrations, and evaluate deformation patterns (Chandra et al., 2024; Davareza et al., 2025). FEA allows for a detailed assessment of the safety factor, ensuring that the design complies with industrial standards for lifting equipment prior to fabrication.

Consequently, this research aims to analyze the structural response of an adjustable spreader carbody under a 40-ton static load by evaluating three material variations: SS400, SM490A, and S355J2+N. Utilizing Autodesk Inventor for 3D modeling and ANSYS Workbench for static structural simulation, this study will assess the maximum Von Mises stress, total deformation, and minimum safety factor. The ultimate objective is to determine the most optimal, safe, and cost-effective material for spreader manufacturing at Perusahaan Kereta Api, thereby enhancing both operational safety and production efficiency (Pilargenta et al., 2024; Widyastuti et al., 2025).

2. THEORETICAL STUDY

Spreader Beam and Lifting Operations in Heavy Industry

The adjustable spreader beam is a critical lifting accessory designed to distribute concentrated loads evenly across multiple lifting points, thereby preventing structural damage to the payload. In heavy industries, such as rolling stock manufacturing, spreaders are essential for handling massive components like Electric Multiple Unit (EMU) car bodies, which can weigh up to 40 tons (Harnany et al., 2024). Telescopic or adjustable spreader bars offer significant operational flexibility, allowing the lifting span to be modified to accommodate varying payload dimensions (Suryawan et al., 2025). However, the structural integrity of the spreader is paramount, as it must withstand complex dynamic and static forces without excessive deformation. Previous studies have emphasized that the failure of lifting equipment can lead to catastrophic accidents, necessitating rigorous design and material evaluation to ensure operational safety (Duarte et al., 2021; Shi et al., 2026).

Material Variation and Structural Steel Properties

The mechanical performance of a spreader beam is heavily dictated by the physical and mechanical properties of the chosen material. Structural steels are predominantly used due to their high tensile strength, ductility, and weldability. This research evaluates three common grades: SS400, SM490A, and S355J2+N. SS400 is a general structural steel widely used for manufacturing lifting handles and frames due to its cost-effectiveness and adequate yield strength of 245 MPa (Haihaogroup, 2025; Ramadhan et al., 2025). SM490A offers higher tensile strength, making it suitable for welded structures requiring greater load-bearing capacity (XTDSTEELSTRUCTUR, 2025). Meanwhile, S355J2+N is a normalized medium-strength steel recognized for its excellent toughness and resistance to fatigue, with a yield strength of 355 MPa (Gangsteel, 2025; Milovanović et al., 2022). The variation in material properties directly influences the stress distribution and deformation behavior under maximum load conditions, a factor that has been proven critical in the design of heavy machinery components and frames (Fahmi et al., 2023; Kiswara & Suryo, 2023; Wokanubun et al., 2023).

Finite Element Analysis (FEA) in Mechanical Design

To evaluate the structural response of the spreader without the prohibitive costs of physical prototyping, Finite Element Analysis (FEA) is employed as a robust computational tool. FEA discretizes complex geometries into finite elements (mesh) to numerically solve differential equations governing stress and displacement (Pierce & Henriksen, 2022). The standard workflow involves 3D modeling using CAD software such as Autodesk Inventor, followed by numerical simulation in environments like ANSYS Workbench (Chandra et al., 2024; Davareza et al., 2025). The application of FEA has been widely validated in various mechanical design optimizations, including the analysis of lifting tools (Pilargenta et al., 2024), heavy equipment buckets (Kiswara & Suryo, 2023), and marine engine mounts (Widyastuti et al., 2025). By simulating static structural conditions, engineers can accurately predict stress concentrations, particularly at geometric discontinuities such as lug holes, and assess the overall stiffness of the structure (Fajrin et al., 2022; Wibawa, 2022).

Evaluation Parameters and Safety Standards

The structural feasibility of the spreader design is assessed using three primary parameters derived from the FEA simulation: Von Mises stress, total deformation, and safety factor. Von Mises stress is utilized to predict the onset of yielding by comparing the equivalent stress to the material's yield strength, ensuring the structure remains within the elastic region. Total deformation measures the deflection of the spreader under load, which must be minimized to maintain payload stability during lifting. Furthermore, the safety factor, defined as the ratio of the material's yield strength to the maximum working stress, is a critical metric for lifting equipment. Industry standards mandate a minimum safety factor between 2.5 and 3.0 to account for dynamic loading, shock loads, and material imperfections (Jaya et al., 2021). By systematically analyzing these parameters across different material variations, the optimal balance between structural safety, weight efficiency, and economic viability can be achieved.

3. RESEARCH METHODS

The adjustable spreader beam is a critical lifting accessory in heavy industries like rolling stock manufacturing, designed to evenly distribute concentrated loads and prevent structural damage to massive payloads such as Electric Multiple Unit (EMU) car bodies weighing up to 40 tons. This study evaluates three structural steel grades SS400 (245 MPa yield strength), SM490A (325 MPa), and S355J2+N (355 MPa) to determine their influence on stress distribution, stiffness, and deformation behavior under maximum load conditions. To avoid costly physical prototyping, Finite Element Analysis (FEA) is conducted using Autodesk Inventor for 3D modeling and ANSYS Workbench for static structural simulation, assessing structural feasibility through Von Mises stress (to predict yielding), total deformation (to ensure payload stability), and safety factor (with industry standards requiring 2.5–3.0 to account for dynamic loading and material imperfections).

4. RESULTS AND DISCUSSION

The simulation was run using the Static Structural analysis type. The computational results were then processed in the post-processing stage to observe the response of the three material types. The simulation data includes the maximum stress (Von Mises stress), maximum deformation (Total Deformation), and the lowest safety factor (Safety Factor Minimum) for the three spreader length variations (3500 mm, 3750 mm, and 4000 mm). The following is a comprehensive description of the results and discussion.

Results

Load Calculation Results

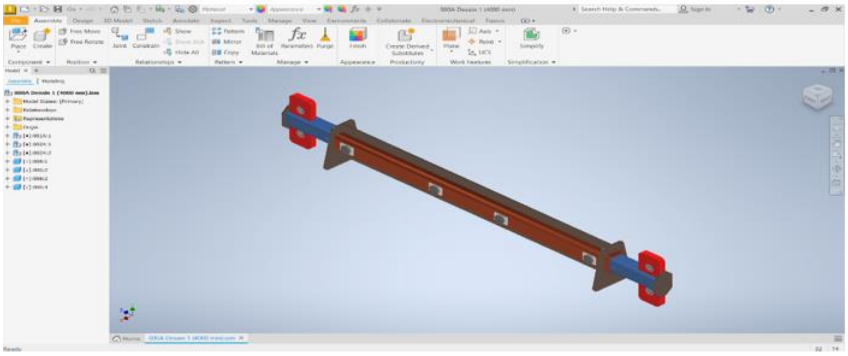

Figure 1. Spreader Design.

Results 1. Spreader Design, to perform a Finite Element Analysis simulation on a spreader, a 40-ton lifting load must be decomposed into horizontal (Fx) and vertical (Fy) forces using sine and cosine functions, because the sling angle changes as the spreader length changes. The spreader has a telescopic mechanism with three length variations, namely 3500 mm, 3750 mm, and 4000 mm, where each change in length produces a different angle so that the Fx and Fy values are also different. Of the three variations, the length of 4000 mm was chosen as the most critical condition because it produces the largest bending moment. Calculations using sin and cos at each length aim to obtain accurate Fx and Fy values as simulation input, so that the results of the von mises analysis, deformation, and safety factor spreader describe the actual lifting conditions.

Finite Element Analysis Simulation

This research applies Finite Element Analysis (FEA) simulation using ANSYS Workbench software, using the static structural analysis method. The aim is to identify changes in the spreader structure due to loading, including von Mises values, deformation, and safety factors.

Simulation Programming Process

After the spreader design was completed, a simulation was conducted using ANSYS Workbench, with stages starting from setting up the engineering data, entering the design geometry, meshing, and entering the variables required for the simulation.

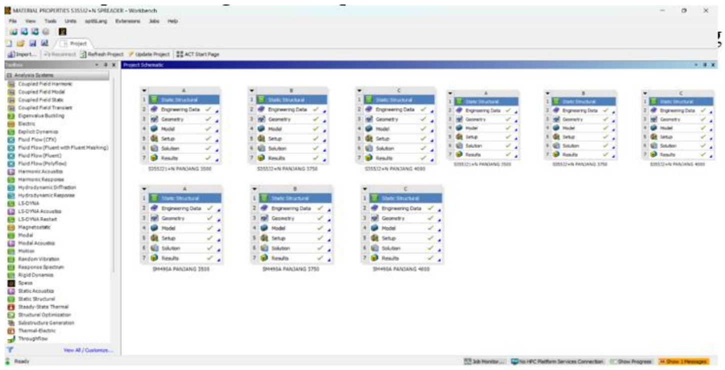

Figure 2. Ansys Worksbench Software Display With Static.

Structural Analysis Systems Table. In this simulation, the Analysis System Static Structural feature of ANSYS Workbench is used as a tool to calculate and analyze the spreader response to loads acting under static conditions.

Engineering Data

At this stage, the type of material to be simulated was selected, where this study used three material variations, namely SS400, SM490A, and S355J2 + N. The property values of each material were entered according to the data that had been obtained so that the material characteristics in the simulation represented the actual condition of the material used in the field.

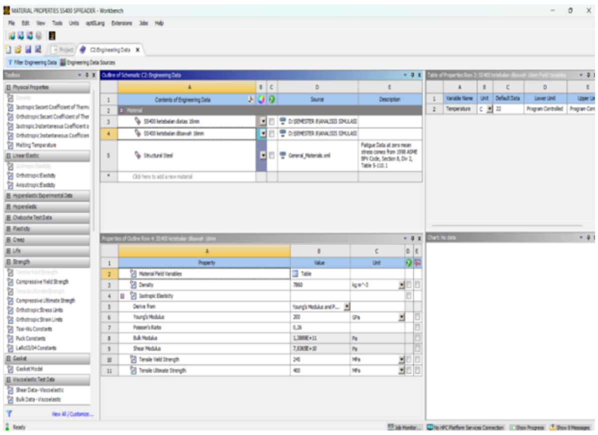

Figure 3. Data Engineering Display.

Geometry

This stage begins by importing the design geometry from Autodesk Inventor into ANSYS Workbench in the STEP file format (*.stp;*.ste;*.step;*.stpz). Geometry checks are performed to ensure design suitability and detect possible geometry problems through ANSYS Workbench software readings.

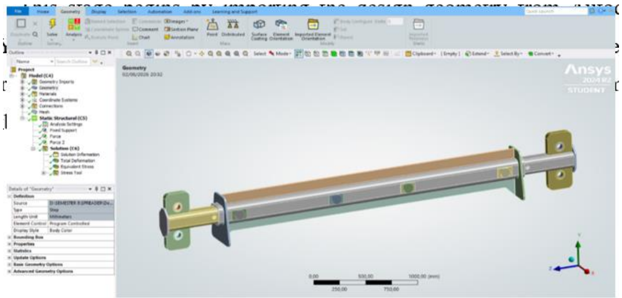

Figure 4. Geometry View.

Model

In the pre-processing stage, geometry checks are carried out, material properties are determined, coordinate system determination, connection arrangements, and meshing processes are carried out on the design geometry. The meshing process is an essential step for numerical simulations to run. In this simulation, the mesh size used is set to 5 mm.

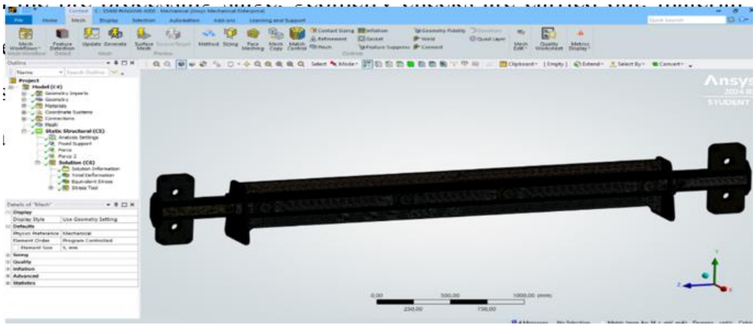

Figure 5. 5 mm Meshing Display On Spreader.

Setup

At the setup stage, identification is carried out to determine which parts will be the support (fixed support) and which parts will be given a load (force). In this spreader design, the base is located on the pedeye with two holes on the top side, as shown in the figure.

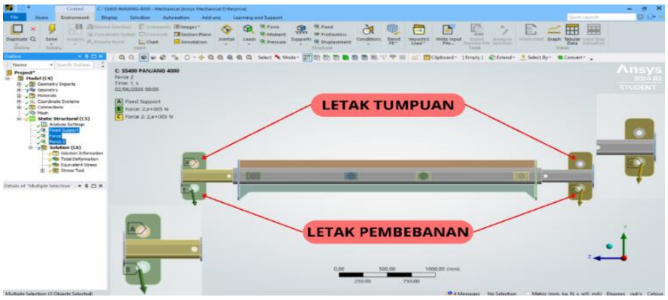

Figure 6. Fixed Support Placement and Force Placement (Loading).

Solution

At the solution stage, a parameter configuration is carried out which will be a reference in determining the output of the simulation calculation results. The parameters set include Equivalent Von Mises Stress, Total Deformation, and Safety Factor. Furthermore, the ANSYS

Workbench software executes a numerical computational process based on those parameters to generate the desired data

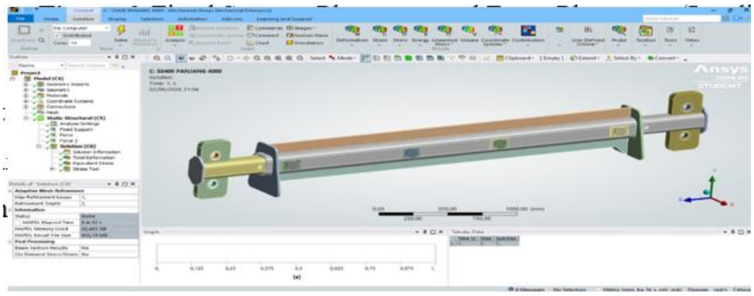

Figure 7. Static Structural Solution View.

Result

At the result stage, all simulation outputs will be presented according to the configuration that has been set at the solution stage. The result data includes a geometric display and a report preview that can be taken as the final result of the simulation process.

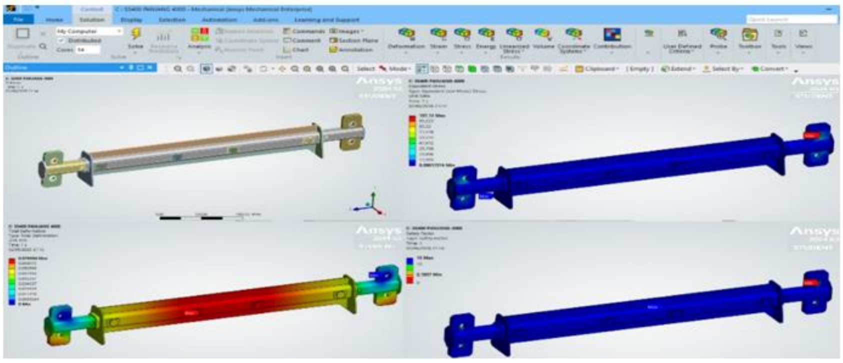

Figure 8. Static Structural Result Display.

Simulation Results

The data that comes out is the result of the simulation process. This output provides a comprehensive overview of the static behavior of the spreader design. The results are then grouped into three main parameters, namely voltage distribution (von misses stress), structure displacement (deformation), and safety factor values (safety factor). In this section, the simulation data for each material variation is presented in detail to facilitate performance evaluation and determine the most optimal and efficient material among the tested variations.

Voltage Distribution Value (Von Misses Stress)

Spreader With Steel Material SS400

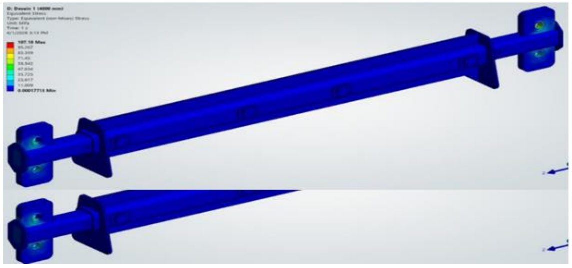

Figure 9. Voltage Distribution of Von Mises Spreader On SS400 Steel.

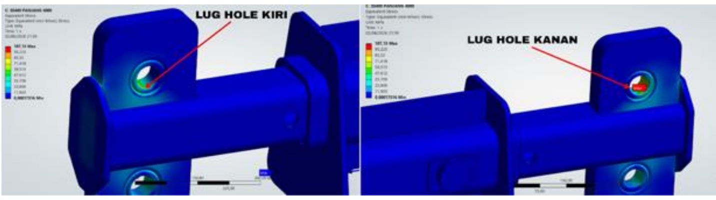

Figure 10. Right and Left Lug Hole Details.

Based on the analysis, the results of the simulation of a spreader with a length of 4000 mm using SS400 steel material showed that the highest von mises voltage was recorded at 107.18 MPa. The location of the maximum tension concentration is found in the area around the lug holes on both sides of the structure, namely the left and right sides. When this value is compared to the yield strength of SS400 material which is in the range of 205 - 245 MPa, then the spreader structure can be declared safe. The tension level that occurs is still far below the limit of material elasticity, so that in the simulated loading condition of 40 tons, the structure is predicted to not experience failure or permanent shape change or plastic deformation.

Spreader With Steel Material SM490A

Figure 11. Voltage Distribution of Von Mises Spreader On SM490A Steel.

Based on the analysis, the results of the simulation on a spreader structure with a span length of 4000 mm using SM490A steel material showed a maximum von mises voltage value of 107 MPa, where the highest voltage concentration point occurred in the cross-sectional area around the lug holes on the left and right sides of the structure due to the stress concentration phenomenon triggered by sudden geometric changes. If this maximum voltage value is compared to the yield strength of SM490A material, which is 325 MPa, then the spreader structure is declared safe because the voltage that occurs is still far below the material elasticity limit with a difference of 218 MPa. Thus, under the conditions of simulated loading of 40 tons, the spreader structure is not expected to experience structural failure or plastic deformation during the lifting process.

Spreader With Steel Material S355J2+N

Figure 12. Voltage Distribution of Von Mises Spreader on S355J2+N Steel.

Based on the simulation results, the 4000 mm spreader structure using S355J2+N steel generates a von Mises stress of 106.96 MPa, with critical stress concentration detected around the lug holes on both sides due to geometric discontinuities. Since this stress value remains significantly below the material's yield strength of 355 MPa—leaving a residual load-bearing capacity of 248.04 Mpa the structure is deemed safe and predicted to withstand the 40-ton lifting load without permanent deformation or structural damage.

Total Deformation Value

Spreader With Steel Material SS400

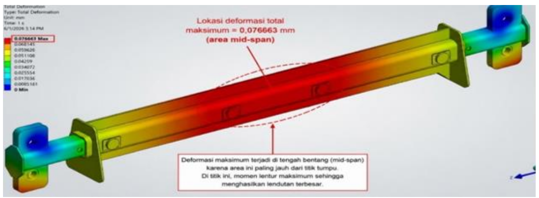

Figure 13. Total Deformation Spreader on SS400 Steel.

Based on the simulation results, the 4000 mm spreader structure using SS400 steel with outer hollow square profiles (200 × 200 × 16 mm) and inner adjustable profiles (160 × 160 × 12 mm) produces a total deformation of 0.076663 mm concentrated at the mid-span— the area farthest from the support points where maximum bending moment naturally occurs. With deformation well below 0.1 mm, the structure maintains excellent geometric stability and demonstrates sufficient stiffness for lifting 40-ton Electric Rail Train (KRL) car bodies, ensuring operational safety throughout the process.

Spreader With Steel Material SM490A

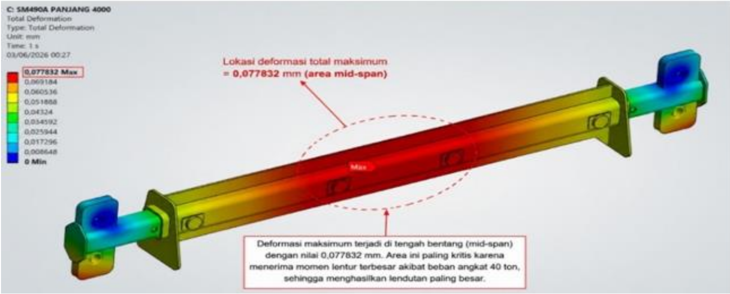

Figure 14. Total Deformation Spreader On SM490A Steel.

Based on the simulation results, the 4000 mm spreader using SM490A steel with outer hollow square profiles (200 × 200 × 16 mm) and inner adjustable profiles (160 × 160 × 12 mm) produced a total deformation of 0.077832 mm at the mid-span the critical location experiencing maximum bending moment under the 40-ton lifting load. With deformation below 0.08 mm, the structure maintains excellent geometric stability, demonstrating that the SM490A material combined with this hollow square profile configuration provides sufficient rigidity for heavy lifting operations, thereby ensuring safety, stability, and precision during KRL carbody lifting in accordance with applicable safety standards.

Spreader With Steel Material S355J2+N

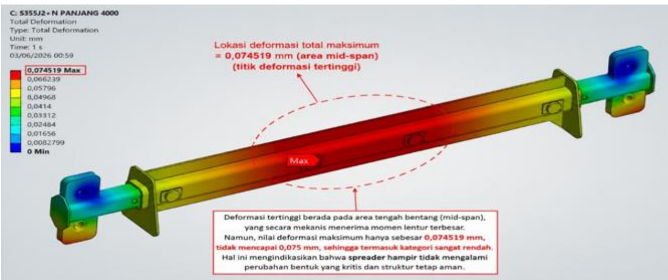

Figure 15. Total Deformation Spreader On Steel S355J2+N.

Based on the simulation results, the 4000 mm spreader using S355J2+N steel with outer hollow square profiles (200 × 200 × 16 mm) and inner adjustable profiles (160 × 160 × 12 mm) produced a total deformation of 0.074519 mm concentrated at the mid-span the structurally weakest point subjected to maximum bending moment. With deformation below 0.075 mm, the structure exhibits negligible shape change, demonstrating exceptional rigidity and integrity under the 40-ton load. Thus, S355J2+N steel proves highly suitable for spreader applications, providing excellent dimensional stability and structural resistance to ensure safe, controllable KRL carbody lifting operations.

Safety Factor Value

Spreader With Steel Material SS400

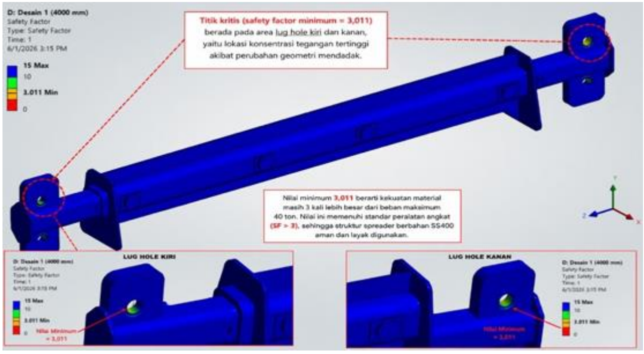

Figure 16. Safety Factor Spreader on SS400 Steel.

Based on the simulation results, the 4000 mm adjustable spreader using SS400 steel achieved a minimum safety factor of 3.011 at the lug holes locations of highest stress concentration due to geometric discontinuities indicating the material strength is three times greater than the simulated 40-ton load. This value exceeds the minimum safety threshold of 3.0 required by lifting equipment standards, confirming operational feasibility and compliance with occupational safety regulations. The maximum safety factor reached 15 in low-stress regions such as the center of the hollow square profile, far from load application points. Thus, the SS400 spreader structure demonstrates sufficient safety margins to withstand potential shock loads and dynamic fluctuations during KRL carbody lifting operations.

Spreader With Steel Material SM490A

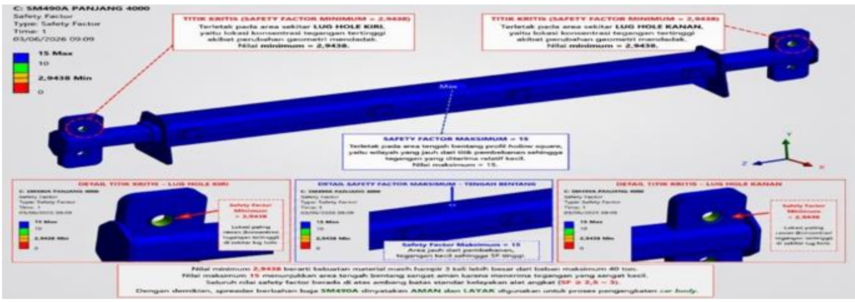

Figure 17. Safety Factor Spreader On SM490A Steel.

Based on the simulation results for the 4000 mm spreader using SM490A steel, the minimum safety factor of 2.9438 was recorded at the lug holes the most vulnerable points due to highest stress concentration. This represents a slight decrease of 0.0672 compared to SS400 (3.011), yet still indicates the material strength is nearly three times the 40-ton maximum load. The maximum safety factor reached 15 at the mid-span of the hollow square profile, where stress is minimal due to distance from loading points. Although marginally lower than SS400, the SM490A safety factor remains within the standard feasibility threshold of 2.5–3.0 for lifting equipment, confirming adequate safety margins to withstand shock loads and sudden load fluctuations during KRL carbody lifting operations.

Spreader With Steel Material S355J2+N

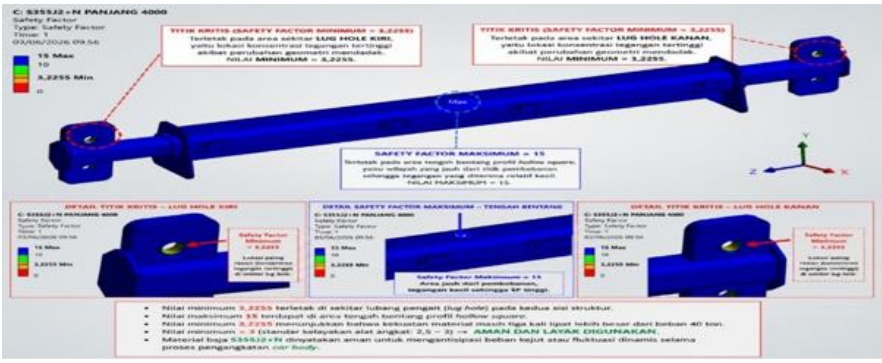

Figure 18. Safety Factor Spreader on S355J2+N Steel.

Based on the simulation results, the 4000mm spreader using S355J2+N steel achieved a minimum safety factor of 3.2255 at the lug holes, surpassing SS400 (3.011) by 0.2145 and SM490A (2.9438) by 0.2817. This indicates the material strength exceeds the 40-ton load by more than threefold. The maximum safety factor reached 15 at the mid-span of the hollow square profile, where stress is minimal. S355J2+N ranks highest in safety performance, followed by SS400 and SM490A, yet all three materials meet the minimum lifting equipment standard of 2.5–3.0, ensuring safe operation against shock loads and dynamic fluctuations during KRL carbody lifting at the Railway Company.

Simulation Results Analysis

Based on the results of data processing from static structural simulations using the FEA (Finite Element Analysis) method on adjustable spreaders, it is presented in the form of tables and graphs. The data displayed included three main structural response parameters, namely von mises stress, total deformation, and safety factor, for each variety of steel material tested (SS400, SM490A, and S355J2+N). This table and graph aims to facilitate the comparison of mechanical performance between materials and is the basis for the discussion of the analysis of spreader strength on material variations with the loading of Electric Rail Train (KRL) carbodies in Railway Companies.

Table 1. Simulation Results of Spreader With 3500 mm Length.

No	Material Type	Von Mises	Deformation	Safety Factor
1	SS400	80,859 Max	0,038123 Max	3,4808 Min
2	SM490A	80,877 Max	0.038613 Max	3,8948 Min
3	S355J2+N	80,889 Max	0,036938 Max	4,2651 Min

The simulation results at a length of 3500 mm show that the S355J2+N material (yield strength 355 MPa, modulus of elasticity 210 GPa) is the most optimal choice for spreaders.

Although all three materials (S355J2+N, SM490A, and SS400) have almost the same von mises stress (80.86–80.89 MPa) due to the equivalent modulus of elasticity, S355J2+N excels with the smallest deformation (0.0369 mm) and the highest safety factor (4.2651). In contrast, the SM490A (yield strength 325 MPa) produces a deformation of 0.0386 mm and a safety factor of 3.8948, while the SS400 (lowest yield strength of 245 MPa) produces a deformation of 0.0381 mm and a safety factor of 3.4808. The difference in yield strength is the main factor that affects the safety factor, so that S355J2+N is the best material with the highest level of safety and maximum rigidity.

Table 2. Simulation Results of Spreader With Length 3750 mm.

No	Material Type	Von Mises	Deformation	Safety Factor
1	SS400	93,598 Max	0,053545 Max	3,3393 Min
2	SM490A	93,518 Max	0.054252 Max	3,3683 Min
3	S355J2+N	93,501 Max	0,051906 Max	3,6898 Min

Based on the simulation results in Table 2, the comparison of the three materials at 3750 mm length shows that the increased spreader length generates greater bending moments, raising von Mises stress to approximately 93.50–93.60 MPa and deformation to 0.0519–0.0543 mm. S355J2+N maintains superior performance with the lowest von Mises stress (93.50 MPa), smallest deformation (0.0519 mm), and highest safety factor (3.6898), enabling the spreader to retain adequate stiffness despite increased stress and deflection. SM490A yields 93.52 MPa stress, 0.0543 mm deformation, and 3.3683 safety factor, while SS400 produces 93.60 MPa stress, 0.0535 mm deformation, and 3.3393 safety factor. S355J2+N remains the optimal choice, as its highest yield strength provides the greatest strength reserve to anticipate load fluctuations during lifting operations.

Table 3. Simulation Results of Spreader With 4000 mm Length.

No	Material Type	Von Mises	Deformation	Safety Factor
1	SS400	107,18 Max	0,076663 Max	3,011 Min
2	SM490A	107 Max	0.077832 Max	2,9438 Min
3	S355J2+N	106,96 Max	0,074519 Max	3,2255 Min

Based on the simulation results in Table 4.3, the comparison of the three materials at the most critical 4000 mm length shows that von Mises stress peaks at 106.96–107.18 MPa and deformation reaches 0.0745–0.0778 mm. S355J2+N demonstrates optimal performance with the lowest von Mises stress (106.96 MPa), smallest deformation (0.0745 mm), and highest safety factor (3.2255), providing sufficient strength to withstand dynamic loads and shocks during lifting. SS400 yields the highest stress at 107.18 MPa with 0.0767 mm deformation and 3.011 safety factor, while SM490A records the lowest safety factor (2.9438) despite comparable stress (107 MPa) and deformation (0.0778 mm). S355J2+N proves the most efficient and optimal material due to its highest yield strength (355 MPa) producing the greatest safety margin under critical conditions, and its highest elastic modulus (210 GPa) resulting in the lowest stress and deformation. Although SS400 and SM490A still meet feasibility standards, S355J2+N offers superior safety performance and is recommended for manufacturing spreaders lifting 40-ton carbodies. Consequently, if the 4000 mm S355J2+N spreader is deemed safe, the same material at 3500 mm and 3750 mm lengths will theoretically achieve even higher safety levels.

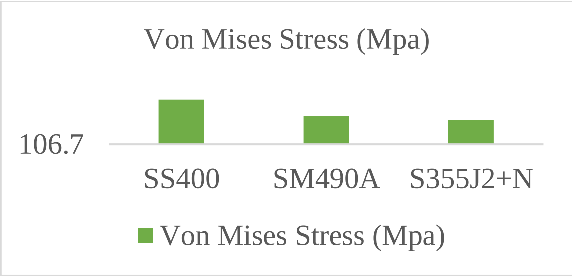

Figure 19. Von Mises Stress (MPa) Spreader Length 4000 mm.

The results of the von mises simulation graph on the 4000 mm long spreader which is the most critical condition with the greatest bending moment, the highest von mises stress occurs at SS400 107.18 MPa because the modulus of elasticity is at the lower limit of the range of 190 GPa, followed by SM490A 107 MPa with an elasticity modulus of 200 GPa, and the lowest at S355J2+N 106.96 MPa because the highest modulus of elasticity is 210 GPa so that the material is stiffer and the tension distribution is more even. The entire tension value is still far below the yield strength of each material, so that the spreader at the maximum span remains safe against plastic deformation and the tension concentration point in the hook hole is still within the safe limit.

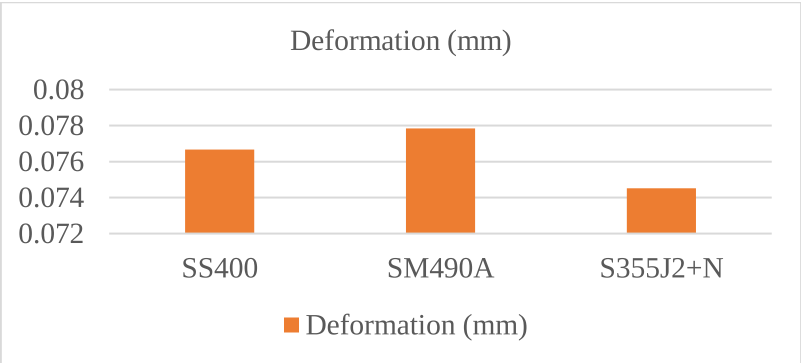

Figure 20. Deformation (mm) Spreader Length 4000 mm

In the deformation graph, the 4000 mm long spreader that produces the most deformation due to deformation is directly proportional to the length of the stretch, the highest deformation value occurs at SM490A 0.077832 mm because the modulus of elasticity is 200 GPa, then SS400 0.076663 mm with an elasticity modulus of 190–210 GPa, and the lowest at

S355J2+N 0.074519 mm because the highest modulus of elasticity is 210 GPa so that the material is the stiffest and resists deflection the best. The entire deformation value is still very small, less than 0.08 mm, so that the spreader at the maximum span is still able to maintain its geometric dimensions very well and the carbody lifting stability is guaranteed.

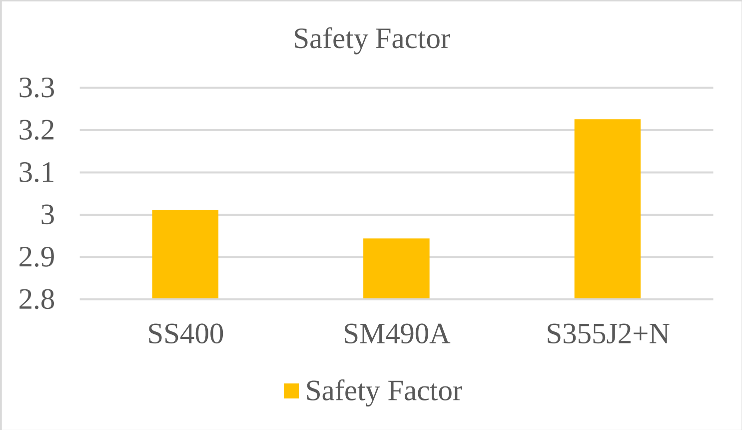

Figure 21. Safety Factor Spreader Length 4000 mm.

Based on the safety factor graph, the 4000 mm long spreader which is the condition with the lowest safety factor because the voltage that occurs is the greatest compared to other lengths, the highest safety factor value occurs at S355J2+N 3.2255 because it has the highest yield strength of 355 MPa, followed by SS400 (3.011) with a yield strength of 245 MPa, and the lowest at SM490A 2.9438 even though it has a yield strength of 325 Mpa, However, the voltage generated is slightly larger. All safety factor values in the maximum span are still above the standard of feasibility of lifting equipment which requires a minimum value of 2.5 to 3, so that the 4000 mm long spreader is declared to remain in a safe position.

Discussion

The simulation results demonstrate that all three material variations (SS400, SM490A, and S355J2+N) exhibit maximum Von Mises stress values ranging from 106.96 MPa to 107.18 MPa under a 40-ton static load at the critical 4000 mm span. These values are significantly lower than the respective yield strengths of the materials, confirming absolute structural safety. This finding aligns with the research by Ghaemifard & Ghannadiasl (2025) and Montes et al (2026), who observed that spreader beams subjected to variable loading maintain stress levels well within the elastic limit, with maximum stress concentrations consistently occurring at geometric discontinuities such as lug holes. Furthermore, Suryawan et al (2025) corroborated this in their design of a telescopic adjustable spreader bar, noting that proper 3D modeling and Finite Element Analysis (FEA) effectively predict stress distribution, ensuring that the structural integrity of lifting accessories is not compromised under maximum operational loads.

In terms of structural stiffness, the total deformation across all materials remained exceptionally low, measuring less than 0.08 mm. The S355J2+N material exhibited the lowest deformation (0.0745 mm) due to its superior modulus of elasticity (210 GPa). This emphasizes the direct correlation between material stiffness and dimensional stability under heavy lifting conditions. This outcome is consistent with the findings of Shen et al (2025), Tadesse & Fatoba (2022) and Tan et al (2020), who demonstrated through FEA that materials with higher elastic moduli significantly minimize deflection in heavy-duty mounting structures. Similarly, Hassan & Saeed (2024) highlighted that maintaining minimal deformation in bending components is crucial to prevent operational inaccuracies, reinforcing that the selected hollow square profile combined with high-stiffness steel effectively preserves the geometric stability of the carbody during transit.

The analysis of the safety factor reveals that material selection profoundly impacts the margin of safety, with S355J2+N achieving the highest value (3.2255), followed by SS400 (3.011) and SM490A (2.9438). All values satisfy the industrial minimum requirement of 2.5 to 3.0 for lifting equipment. This supports the conclusions drawn by Changxu & Yisheng (2024) and Xiao (2021), who found that varying materials in heavy equipment buckets directly dictates the safety factor, with higher yield strength steels providing a more robust buffer against unexpected load spikes. Additionally, Wokanubun et al (2023) reported similar trends in UAV cargo box structures, where material variation was the primary determinant of structural reliability. The current study validates that while all tested steels are viable, S355J2+N offers the most substantial mechanical reserve against dynamic shock loads.

Despite the mechanical superiority of S355J2+N, the practical application in industrial manufacturing must also consider economic efficiency. The study identifies SS400 as the most optimal and cost-effective choice, as it comfortably meets the safety factor threshold (3.011) while offering lower material costs and broader market availability. This practical trade-off is supported by Ramadhan et al (2025), who successfully utilized SS400 in the manufacturing of lifter handles, concluding that its adequate yield strength (245 MPa) provides a highly economical solution without sacrificing operational safety.

Furthermore, Chandra et al (2024) emphasized that optimizing production processes requires balancing technical performance with manufacturing efficiency, suggesting that over-specifying materials (e.g., using S355J2+N when SS400 is sufficient) can lead to unnecessary production costs. While the static structural analysis provides a comprehensive evaluation of the spreader's capacity under a 40-ton load, it is important to acknowledge the limitations of static modeling in real-world lifting scenarios. Lifting operations inherently involve dynamic forces, such as crane acceleration, deceleration, and payload swinging. Future research should expand upon this foundation by incorporating dynamic analysis and fatigue life calculations. This recommendation is strongly supported by Milovanović et al (2022), who highlighted the critical importance of evaluating the fatigue behavior of steels like S355J2+N under cyclic loading conditions. Similarly, Davareza et al (2025) advocated for advanced FEA simulations in railway components to capture complex, real-world loading spectra, indicating that dynamic and fatigue analyses are essential next steps to ensure the long-term durability of the spreader carbody.

4. CONCLUSION

This study concludes that the adjustable spreader carbody designed for 40-ton EMU trains is structurally safe across all tested material variations (SS400, SM490A, and S355J2+N) at its most critical span of 4000 mm. Finite Element Analysis (FEA) revealed that all materials exhibited maximum Von Mises stresses below 107.18 MPa, minimal total deformations under 0.08 mm, and safety factors ranging from 2.94 to 3.22, successfully meeting the industrial lifting standard requirement of 2.5 to 3.0. Although S355J2+N demonstrated the highest mechanical performance with the lowest deformation, SS400 is ultimately recommended as the most optimal and efficient material for manufacturing at PERUSAHAAN KERETA API. This recommendation is based on SS400's ability to provide an adequate safety margin (3.011) while offering superior cost-effectiveness and widespread market availability, ensuring safe, reliable, and economical lifting operations without compromising structural integrity.

REFERENCES

Chandra, M. A., Isminarti, I., Fauziah, F., Mulyadi, Y. B., & Abas, M. I. (2024). Optimizing production process by integrating 3D manufacturing technology using Autodesk Inventor software to improve efficiency. *Jurnal Ilmu Komputer (JUIK)*, *4*(3), 144. https://doi.org/10.31314/juik.v4i3.3460

Changxu, S., & Yisheng, S. (2024). Strengthening of metal. *The ECPH Encyclopedia of Mining and Metallurgy*, 2048–2057. https://doi.org/10.1007/978-981-99-2086-0_1054

Davareza, T., Nataria, A., Ganda, F., Wulandari, D., Mubarok, D. D., & Firmansyah, G. P. (2025). Studi finite element analysis terhadap kekuatan struktural dua desain roda kereta menggunakan ANSYS Workbench 17.2. *Jurnal [Tidak Diketahui]*, *10*(3), 628–637.

Duarte, J., Torres Marques, A., & Santos Baptista, J. (2021). Occupational accidents related to heavy machinery: A systematic review. *Safety*, *7*(1), 21. https://doi.org/10.3390/safety7010021

Efinger, D., Ostertag, A., Dazer, M., Borschewski, D., Albrecht, S., & Bertsche, B. (2022). Reliability as a key driver for a sustainable design of adaptive load-bearing structures. *Sustainability*, *14*(2), 895. https://doi.org/10.3390/su14020895

Fahmi, R., Zaenudin, M., & Saleh, Y. (2023). Berdasarkan variasi material pada prototipe. *TECHNOPEX*, (2022), 32–48.

Fajrin, M. G. F. G., Widiantoro, H., & Zainuddin, Z. (2022). Analisis elemen hingga bagian penekuk pada mesin pembuat begel baja tulangan 8 mm. *Suara Teknik: Jurnal Ilmiah, 13*(1), 8. https://doi.org/10.29406/stek.v13i1.4222

Gangsteel. (2025). *What are the properties of EN 10025 S355J2*. https://gangsteel.net/News/What_are_the_properties_of_EN_10025_S355.html

Ghaemifard, S., & Ghannadiasl, A. (2025). A review of moving-load dynamic problems: Specialized modeling for beam and plate vibrancy. *Journal of Vibration Engineering & Technologies*, *13*(5), 280–. https://doi.org/10.1007/s42417-025-01837-2

Haihaogroup. (2025). *JIS G3101 general structure hot rolled SS400 steel*. https://www.haihaopiping.com/jis-g3101-general-structure-hot-rolled-ss400-steel.html

Harnany, D., Adista, R. K. A., Syaifudin, A., Putra, A. B. K., & Priyambodo, S. (2024). Strength consideration on car body modification for panoramic train. *Jurnal Rekayasa Mesin*, *15*(1), 355–366. https://doi.org/10.21776/jrm.v15i1.1510

Hassan, H. Z., & Saeed, N. M. (2024). Advancements and applications of lightweight structures: A comprehensive review. *Discover Civil Engineering*, *1*(1), 47. https://doi.org/10.1007/s44290-024-00049-z

Jaya, R., Astuti, E. T., & Rohmat, N. (2021). Simulasi desain roller sebagai komponen track tumpuan rantai prototipe excavator untuk menentukan kekuatan material menggunakan Autodesk Inventor. *Jurnal Inovasi Ilmu Pengetahuan dan Teknologi*, *3*(1), 31. https://doi.org/10.32493/jiptek.v3i1.24709

Kiswara, J. P. I., & Suryo, S. H. (2023). Analisis kekuatan bucket dan gaya statis pada bucket backhoe John Deere 310L terhadap variasi material. *Jurnal [Tidak Diketahui]*, *11*(1), 255–264.

Kljaić, Z., Pavković, D., Cipek, M., Trstenjak, M., Mlinarić, T. J., & Nikšić, M. (2023). An overview of current challenges and emerging technologies to facilitate increased energy efficiency, safety, and sustainability of railway transport. *Future Internet*, *15*(11), 347. https://doi.org/10.3390/fi15110347

Milovanović, V., Arsić, D., Milutinović, M., Ž., M., & T., M. (2022). A comparison study of fatigue behavior of S355J2+N, S690QL and X37CrMoV5-1 steel. *Metals*, 12(7), Article 1199. https://doi.org/10.3390/met12071199

Montes, H., Xue, C., Wang, S., Wang, X., Mao, P., & Duan, M. (2026). Experimental investigation of the dynamic behavior of welded-plate lifting lugs for hoisting large-span steel cap beams. *Buildings*, *16*(2), 370. https://doi.org/10.3390/buildings16020370

Oswald, D., Ahiaga-Dagbui, D. D., Sherratt, F., & Smith, S. D. (2020). An industry structured for unsafety? An exploration of the cost-safety conundrum in construction project delivery. *Safety Science*, *122*, 104535. https://doi.org/10.1016/j.ssci.2019.104535

Pierce, E. N., & Henriksen, L. (2022). The application of finite element analysis in mechanical design optimization. *International Academic Journal of Innovative Research, 9*(4), 13–18.

Pilargenta, H., Maharani, C. P., Daru Fathur, M. R., Ausin Al Qoroni, M., & Adyono, N. (2024). Analisa faktor keamanan pada desain alat die cut menggunakan simulasi finite element analysys. *Jurnal [Tidak Diketahui], 1*(1), 144–155.

Ramadhan, A. R. A., Muchlis, A., & Fajar, P. A. T. (2025). Manufaktur handle lifter dengan material SS400. *Venus: Jurnal Publikasi Rumpun Ilmu Teknik, 3*(2), 57–68. https://doi.org/10.61132/venus.v3i2.715

Shen, B., Shi, D., & Zhang, M. (2025). Optimization for powertrain mounts of a heavy-duty truck based on the mounts with adjustable stiffness. *International Journal of Automotive Technology, 26*(6), 1431–1445. https://doi.org/10.1007/s12239-025-00239-3

Shi, X., Fu, K., Qiao, Y., Santos, J., & Yuan, Z. (2026). Accident cause analysis for lifting prefabricated components of assembled buildings based on hybrid simulation technology from human factor perspective. *Engineering, Construction and Architectural Management, 33*(1), 578–601. https://doi.org/10.1108/ECAM-04-2024-0431

Suryawan, W., Basuki, P., S, C. W., P, J. J., & Sagaf, M. (2025). Desain adjustable spreader bar telescopic menggunakan ANSYS. *Jurnal Penelitian Rumpun Ilmu Teknik, 4*(3), 1–11. https://doi.org/10.55606/juprit.v4i3.5432

Tadesse, B. A., & Fatoba, O. (2022). Theoretical and finite element analysis (FEA) of coated composite leaf spring for heavy-duty truck application. *Materials Today: Proceedings, 62*, 4283–4290. https://doi.org/10.1016/j.matpr.2022.04.782

Tan, B., Chen, Y., Liao, Q., Zhang, B., Zhang, N., & Xie, Q. (2020). A condensed dynamic model of a heavy-duty truck for optimization of the powertrain mounting system considering the chassis frame flexibility. *Proceedings of the Institution of Mechanical Engineers, Part D: Journal of Automobile Engineering, 234*(10–11), 2602–2617. https://doi.org/10.1177/0954407020909241

Tang, Y., Li, X., & Yu, Y. (2026). Breaking rework chains in low-carbon prefabrication: A hybrid evolutionary scheduling framework. *Buildings, 16*(5), 968. https://doi.org/10.3390/buildings16050968

Wibawa, L. A. N. (2022). Analisis frekuensi natural rangka main landing gear pesawat UAV menggunakan Ansys Workbench. *Jurnal Mesin Nusantara, 5*(1), 65–73. https://doi.org/10.29407/jmn.v5i1.17580

Widyastuti, I. I., Mudjiono, U., Haris, M., Kurniawan, P., Nur, A., & Maulidhia, A. (2025). Analisis kekuatan dudukan kamar mesin kapal dengan metode elemen hingga. *Jurnal [Tidak Diketahui], 4*(2), 0–5. https://doi.org/10.56211/blendsains.v4i2.1289

Wokanubun, D. A., Sofyan, E., Setiawan, F., & Adam, K. (2023). Perancangan dan analisis kekuatan struktur cargo box UAV VTOL terhadap variasi material dan beban menggunakan finite element analysis. *Teknika STTKD: Jurnal Teknik, Elektronik, Engine, 9*(2), 244–255. https://doi.org/10.56521/teknika.v9i2.938

Xiao, Y. (2021). Development of structural testing equipment for impact and complex loading. *Journal of Structural Integrity and Maintenance, 6*(1), 1–15. https://doi.org/10.1080/24705314.2020.1823559

XTDSTEELSTRUCTUR. (2025). *SM490A steel: Composition, properties, and applications*. https://xtdsteel.com/blogs/sm490a-steel-properties-guide/

Xu, J., Zhu, X., Kang, R., Zhang, G., Zheng, Y., Li, J., Chen, G., Dong, Z., & Cui, H. (2025). Micro-macro synergy in porous aerostatic bearings: Design, analysis, fabrication, and performance evaluation. *The International Journal of Advanced Manufacturing Technology*, *139*(5), 2161–2192. https://doi.org/10.1007/s00170-025-16080-y

Zhao, H., Liang, J., & Liu, C. (2020). High-speed EMUs: Characteristics of technological development and trends. *Engineering*, *6*(3), 234–244. https://doi.org/10.1016/j.eng.2020.01.008